

## WALL SURFACE TEMPERATURE AS AN INDICATOR OF THE CHANGES IN CAVE AIRFLOW ON THE EXAMPLE OF THE VENTILATION BRANCH IN THE BALCARKA CAVE (MORAVIAN KARST)

POVRCHOVÁ TEPLOTA STĚN JAKO INDIKÁTOR ZMĚN PROUDĚNÍ VZDUCHU JESKYNÍ  
NA PŘÍKLADU VENTILAČNÍ VĚTVE V JESKYNI BALCARKA (MORAVSKÝ KRAS)

MAREK LANG, TEREZA PTÁČNÍKOVÁ, JINDŘICH ŠTELCL

### *Abstract*

Lang, M., Ptáčnicková, T., Štelcl, J., 2026: Wall surface temperature as an indicator of the changes in cave airflow on the example of the ventilation branch in the Balcarka Cave (Moravian Karst). - *Acta Musei Moraviae, Scientiae geologicae*, 111, 1, 103-116 (with Czech summary).

*Wall surface temperature as an indicator of the changes in cave airflow on the example of the ventilation branch in the Balcarka Cave (Moravian Karst)*

Seasonal variations of wall surface temperature in the ventilation branch of the Balcarka Cave (Moravian Karst) were studied focused on their relationship to changes in cave airflow. Long-term monitoring of differences between external and cave air temperatures showed dynamic airflows that can be divided into downward (DAF mode) and upward (UAF mode) airflows. Switch between DAF and UAF modes occurred in late fall or early spring, corresponding to the transitional mode, however, it also occurred during peak DAF/UAF modes. Temperatures of the wall surface in the lower part of the ventilation branch were found to be systematically higher than temperatures in the upper part of the branch. The principal reason is heat transfer between the cave air and the walls. While warm external air contributed to a general temperature increase during DAF mode, cool external/cave air resulted in a significant temperature decrease during UAF mode. However, this pattern could be disrupted by short-term changes in cave ventilation induced both naturally (ventilation mode switching) and anthropogenically (visiting route modification).

*Key words:* Balcarka Cave, cave airflow, IR thermometer, temperature difference, wall surface temperature

Marek Lang, Department of Geological Sciences, Faculty of Science, Masaryk University, Kotlářská 2, 602 00 Brno; e-mail: mareklang@mail.muni.cz

Tereza Ptáčnicková, Department of Biology, Faculty of Education, Masaryk University, Poříčí 623/7, 603 00 Brno

Jindřich Štelcl, Department of Biology, Faculty of Education, Masaryk University, Poříčí 623/7, 603 00 Brno

### INTRODUCTION

The air exchange between external and cave atmospheres represents an important phenomenon that influences (1) cave microclimatology (de FREITAS and LITTLEJOHN, 1987; FAIRCHILD *et al.*, 2006) and (2) various karst processes such as limestone dissolution (e.g. STUMM and MORGAN, 1996), calcite speleothem formation (e.g. BANNER *et al.*, 2007; FRISIA *et al.*, 2011), or speleothem corrosion (e.g. FAIMON *et al.*, 2006) via controlling cave  $P_{CO_2}$  (BALDINI *et al.*, 2008). In principle, cave airflow depends on cave geometry. Two

major types can be distinguished: (i) *static caves*, characterized by one or more entrances at similar altitudes, and (ii) *dynamic caves* with two or more entrances at different altitudes. Resulting air circulation is a product of pressure differences derived from contrasting air densities of both external and cave atmosphere (DE FREITAS *et al.*, 1982). Since air density is primarily controlled by temperature, cave airflows are mostly related to temperature differences

$$\Delta T = T_{\text{air}}^{\text{ext}} - T_{\text{air}}^{\text{cave}}, \quad (1)$$

where  $T_{\text{air}}^{\text{ext}}$  is the external air temperature and  $T_{\text{air}}^{\text{cave}}$  is the cave air temperature [°C] (BUECHER, 1999; PFLITSCH and PIASECKI, 2003; KOWALCZK and FROELICH, 2010). Whereas static caves are ventilated for only half of the season (ŽDÍMAL, 2014, 2015), dynamic caves ventilate throughout the entire year by so-called chimney effect (FAIMON and LANG, 2013). Based on the  $\Delta T$  sign, three ventilation regimes can be distinguished in dynamic caves. While downward airflows corresponding to the downward airflow (DAF) ventilation mode are typical during periods with positive  $\Delta T$  values, upward airflows corresponding to the upward airflow (UAF) ventilation mode occur in the cave during periods with negative  $\Delta T$  values. The regime with airflow direction oscillating between both modes is referred to as a transitional ventilation mode. Stability of the actual ventilation mode allows us to define two different ventilation periods in a dynamic cave: *period of active ventilation* and *period of stagnant ventilation*. During the active ventilation period, the cave stays in either DAF or UAF mode and exchanges its air intensively with the exterior. In contrast, only the cave entrance passages are vented (influenced by exterior) during the stagnant ventilation period.

Previous works on airflow in caves in the Moravian Karst were focused on (1) direct airflow monitoring (e.g. FAIMON *et al.*, 2012; FAIMON and LANG, 2013) and (2) monitoring of CO<sub>2</sub> concentrations in cave atmosphere as a tracer for ventilation (e.g. LANG *et al.*, 2015a, b; LANG *et al.*, 2017). In this context, however, the main indicator of airflow velocity is considered to be radon activity in cave atmosphere due to its constant production and decay (DUEÑAS *et al.*, 2005, 2011; BATIOU-GUILHE *et al.*, 2007; GREGORIČ *et al.*, 2013). In this study, we discuss the impact of airflow on the temperature of the wall surface based on a new dataset from the Balcarka Cave (Moravian Karst), particularly from its separate Exit ventilation branch (EVB). The main goal of this study was to assess the potential of surface temperature of cave walls for cave airflow estimates based on the extent of individual ventilation modes and seasonal distribution of wall surface temperatures throughout the EVB. The study aims to increase the number of indicators used for indirect monitoring of airflow in Moravian Karst caves and beyond, and help in better understanding the airflow in the Balcarka Cave.

## SITE OF STUDY

The study was conducted in the Balcarka Cave located in the northern part of the Moravian Karst near the village of Ostrov u Macochy (Fig. 1). Based on the climate classification by KOTEK *et al.* (2006), Moravian Karst has moderately warm (mean annual temperature of 8.3 °C) and moderately humid (mean annual rainfall of 543 mm) climate with drier and warmer sites in its southern part. Balcarka Cave is formed in Upper Devonian limestones of the Macocha Formation. It consists of narrow corridors with a total length of 1,150 m, connecting chambers with rich speleothem decoration spread over two levels, with a height difference of about 20 m. The overburden thickness reaches up to 40 m, and is likely the same between the levels of the lowest opening (444.3 m) and the highest opening (483.2 m) (LANG *et al.*, 2015b). The presence of three known entrances and some presumed hidden openings in distinct altitudes allows the dynamic behavior of cave air circulation. The cave is open to tourists and had a moderate average attendance of 30,820 persons per year for the period between 2006 and 2024 (OUHRABKA, 2025).

EVB located between the Discoverers' Chimney and the Main exit was chosen as the monitoring area. The area was divided into two passages: (1) the Upper branch passage (UBP) between the Discoverers' Chimney and the Old exit and (2) the Lower branch passage (LBP) between the Old exit and the Main exit (Fig. 1). To cover the entire monitoring area, eight monitoring sites were chosen in both the UBP and the LBP (each of them included four sites). A summary of individual sites is given in Table 1.

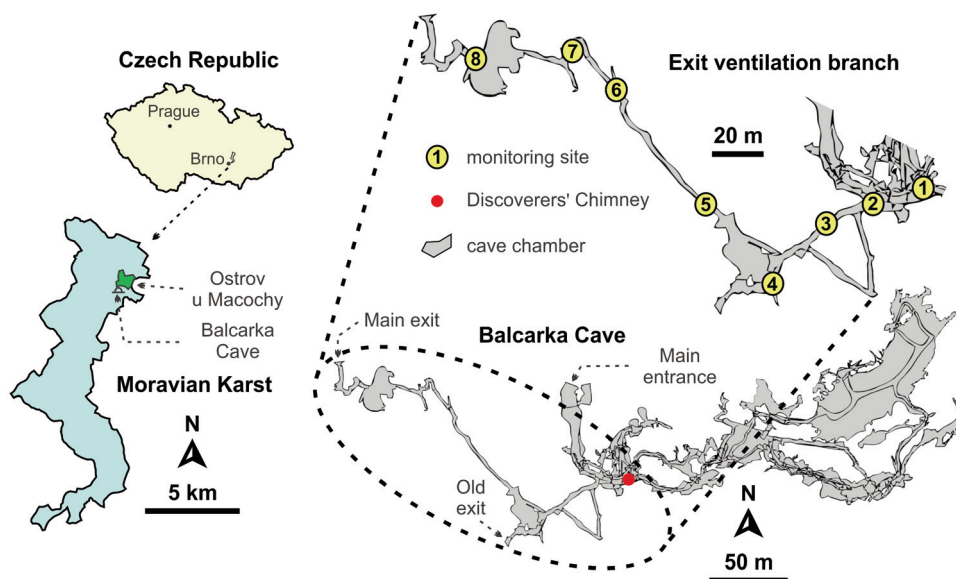


Fig. 1. Site of study: the position and a map of the Balcarka Cave. The numbers denote monitoring sites (see Table 1).

Obr. 1. Místo studia: pozice a mapa jeskyně Balcarka. Čísla označují monitorovací místa (viz tabulka 1).

Tabulka 1. Characteristic of the monitoring sites in the Balcarka Cave (Moravian Karst).

Table 1. Charakteristika monitorovacích míst v jeskyni Balcarka (Moravský kras).

Site	Description	Abbreviation	Position	Character
#1	Discoverers' Chimney	DC	UBP	chamber
#2	Adit-Start	A-S	UBP	corridor
#3	Stalactite Handžár	SH	UBP	chamber
#4	Electrical switchboard	ES	UBP	corridor
#5	Adit-End	A-E	LBP	corridor
#6	Staircase	S	LBP	corridor
#7	Spiral staircase	SS	LBP	corridor
#8	Muzeum Chamber	MC	LBP	chamber

## MATERIALS AND METHODS

Data submitted in this study were collected during (1) regular single measurements in the period from May 2023 to August 2024 and (2) a long-term monitoring campaign covering the entire monitored period. The main monitoring included sixteen single monthly measurements of surface temperature of both right,  $T_{RW}^{cave}$ , and left,  $T_{LW}^{cave}$ , cave walls (in direction from the DC site to the MC site).  $T_{RW}^{cave}/T_{LW}^{cave}$  values at individual sites were measured at three positions (0.5, 1.0, and 1.5 m above the cave floor) and the mean value was calculated. We used BOSCH PTD1 IR thermometer with a measuring range from -20 to 200 °C and a relative error of  $\pm 4.25\%$  from the measured value (LANG *et al.*, 2025). The reason for a non-contact sensor selection was its relative accuracy together with its ability for monitoring of surface temperature of cave walls also in inaccessible cave passages. Based on the manufacturer's recommendation, the thermometer emissivity was set to 0.95 corresponding to the typical value of calcite that forms the cave walls (MINEO and PAPPALARDO, 2021). To correct these data, the measurement in August 2023 was supplemented by a calibrated contact thermocouple FTA104PH (measuring range from -50 to 500 °C, accuracy of  $\pm 2.5$  °C) linked to the ALMEMO 2290-4 V5 Ahlborn data logger (Germany). Values of  $T_{RW}^{cave}/T_{LW}^{cave}$  measured by both IR thermometer and the contact thermocouple were consecutively plotted against each other and fitted by regression lines with the same equation for both the right and left wall

$$T_{CWS}^{cave} = 0.2 T_{RW/LW}^{cave} + 9.3, \quad (2)$$

representing a calibration equation for corrected wall surface temperatures,  $T_{CWS}^{cave}$ . The reasons for a summary calibration equation covering all monitoring sites were (i) a relatively simple geometry of the EVB and (ii) the similar seasonal trends of  $T_{CWS}^{cave}$  observed at selected sites by Ptáčnicková (2025) during previous monitoring. Additional long-term monitoring was focused on  $T_{air}^{ext}$  and  $T_{air}^{cave}$ . While  $T_{air}^{ext}$  was measured approximately 10 m from the Main entrance,  $T_{air}^{cave}$  was logged at the DC site representing the homothermic zone of the cave. For temperature monitoring, Termio-2 data loggers (measuring range from -10 to 100 °C, accuracy of  $\pm 0.07$  °C) were used.

## RESULTS

The  $T_{CWS}^{cave}$  from individual passages of EVB together with the temperature difference  $\Delta T = T_{air}^{ext} - T_{air}^{cave}$  are presented in Figs. 2 and 3. The  $T_{RW}^{cave}/T_{LW}^{cave}$  values show a strong variability depending on cave airflow direction, resulting from  $T_{air}^{ext}$ , ranging between -12.9 and 32.8 °C, and cave airflow direction (Figs. 2a, b and 3a, b). Based on  $T_{air}^{cave}$  varying in a narrow range from 8.6 to 12.0 °C (the mean  $T_{air}^{cave} \sim 9.8$  °C), temperature difference  $\Delta T$  ranged from -22.7 to 23.0 °C (Figs. 2c and 3c). Positive values of  $\Delta T$  correspond to downward airflows, DAF mode (periods from May to early October 2023 and late March to late July 2024), and negative values correspond to upward airflows, UAF mode (periods from November 2023 to early March 2024 and 17 to 25 April 2024). Boundaries between DAF/UAF modes, characterized by rapid mode switching, correspond to the transitional mode (periods of October 2023 and March 2024) (FAIMON *et al.*, 2012).

$T_{CWS}^{cave}$ , varying from 9.2 to 11.8 °C, showed almost identical values (maximal differences up to 0.1 °C) between the right/left walls at individual sites. However, different temperature patterns were identified for sites located in the upper and lower passages of the EVB. Based on  $T_{CWS}^{cave}$  evolution, two distinct phases can be identified in the sites of the upper EVB passage. The first phase, covering the initial year of the monitoring period, showed relatively constant values of approximately 11.7 °C with a deep local minimum of 10.3 °C in August 2023, followed by a systematic decrease to 10.4 °C. At the DC site, a decreasing trend was disrupted by a sharp increase up to 11.4 °C in the period of January/February 2024. In contrast, the second phase was characterized by a more complex evolution of  $T_{CWS}^{cave}$  including two cycles of decrease followed by an immediate increase. Although the initial cycle

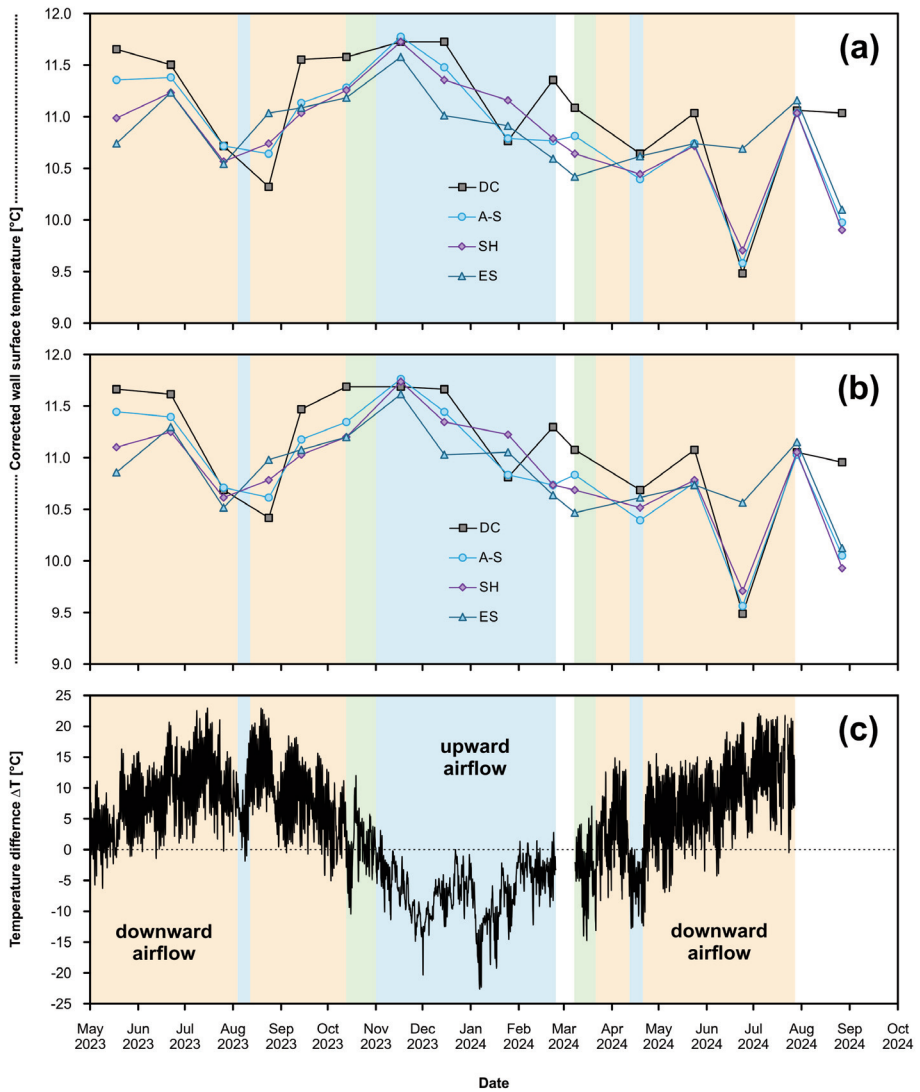


Fig. 2. Long-term data from the upper passage of the Exit ventilation branch in the Balcarka Cave: corrected temperature of the right (a) and left (b) wall surface at individual monitoring sites in dependence on the temperature difference  $\Delta T$  (c). Positioning of walls corresponds to the direction from the DC site towards the MC site. Abbreviations for monitoring sites are consistent with Table 1.

Obr. 2. Dlouhodobá data z horní části Výstupní ventilační větve v jeskyni Balcarka: opravená povrchová teplota pravých (a) a levých (b) stěn na jednotlivých monitorovacích místech v závislosti na teplotním rozdílu  $\Delta T$  (c). Umístění stěn odpovídá směru z DC směrem k MC. Zkratky pro monitorovací místa jsou konzistentní s tabulkou 1.

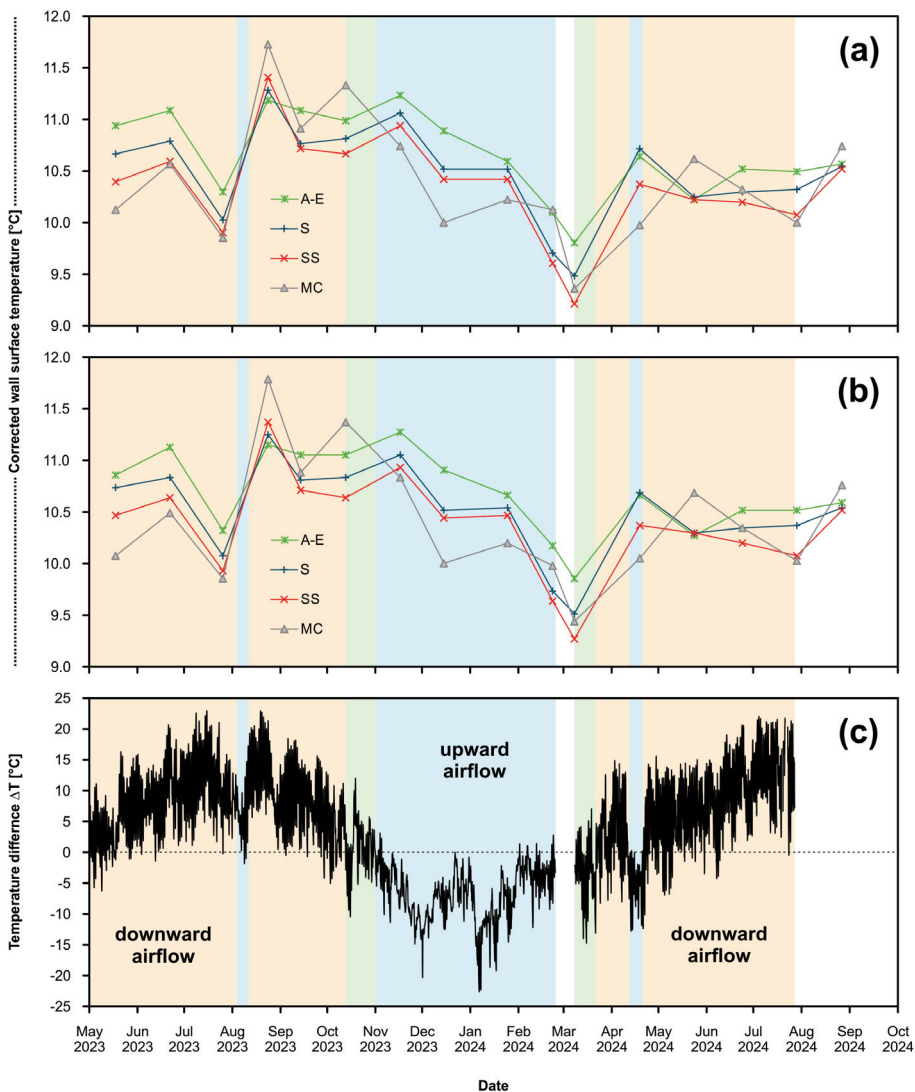


Fig. 3. Long-term data from the lower passage of the Exit ventilation branch in the Balcarka Cave: corrected temperature of the right (a) and left (b) wall surfaces at individual monitoring sites in dependence on the temperature difference  $\Delta T$  (c). Positioning of walls corresponds to the direction from the DC site towards the MC site. Abbreviations for the monitoring sites are consistent with Table 1.

Obř. 3. Dlouhodobá data ze spodní části Výstupní ventilační větve v jeskyni Balcarka: opravená povrchová teplota pravých (a) a levých (b) stěn na jednotlivých monitorovacích místech v závislosti na teplotním rozdílu  $\Delta T$  (c). Umístění stěn odpovídá směru z DC směrem k MC. Zkratky pro monitorovací místa jsou konzistentní s tabulkou 1.

was associated only with a slight increase of 0.3 °C, the subsequent decline and both increases and decreases during the final cycle showed sharp peaks with changes of 1.3 to 1.6 °C. However, it is important to note that there were also some deviations from the above-mentioned pattern, such as the absence of a decrease during the initial/final cycle at the ES/DC sites.

Similar to the upper EVB passage, complex evolution of  $T_{CWS}^{cave}$  was also observed at sites in the lower EVB passage (Figs. 3a, b). It was characterized by two cycles with similar sequence comprising a relatively deep minimum, a sharp increase, and a short-term plateau. During the first cycle, the initial temperature minimum decreased from 10.1 °C (MC site) and 10.9 °C (A-E site) to 9.9 °C (MC site). At the S, SS, and MC sites, this long-term decrease was divided into two parts by a plateau of 10.4 and 10.5 °C (S and SS sites) or an increase by 0.2 °C (MC site) in the period of December 2023/January 2024. It was followed by an immediate increase up to 11.8 °C (MC site) and by stabilization of the temperature around the mean value of 11.0 °C. After a slight decrease of almost 1.0 °C, a second temperature minimum reaching 9.2 °C (SS site) was recorded, followed by a subsequent increase up to 10.7 °C (A-E and S sites). In the final phase of the cycle, the temperatures varied about a mean value of 10.4 °C.

## DISCUSSION

### Seasonality of cave airflow

$T_{CWS}^{cave}$  is generally considered to be in equilibrium with the cave air temperature (BADINO, 2010), which is significantly affected by airflow (LUETSCHER and JEANNIN, 2004; GREGORIĆ *et al.*, 2013). In principle, cave airflows are controlled by external temperature. According to the external temperature, two ventilation periods with opposite airflow directions were historically classified in dynamic caves: (i) summer airflow and (ii) winter airflow (de FREITAS *et al.*, 1982; SPÖTL *et al.*, 2005). In our opinion, this classification, which considers only two periods with specific temperature conditions throughout the entire season, is somewhat questionable, because external temperature varies quite widely and individual summer/winter seasons often contain short-term periods with significantly decreased/increased values. An example of such a period was recorded in April 2024, when a significant drop in external temperatures was identified despite the relatively stable summer season (Figs. 2c and 3c). During this 10-day period, the mean external temperature decreased by almost 9 °C up to -3.1 °C, which indicates a switch from DAF mode into UAF mode. Therefore, it seems more appropriate to use the sign of the  $\Delta T$  values to distinguish the direction of cave airflows, as proposed by FAIMON *et al.* (2012).

Based on the sign of  $\Delta T$  values, five periods with different ventilation modes were distinguished: two periods of DAF mode, two periods of the transitional mode, and one period of UAF mode (Figs. 2 and 3). The presence of DAF/UAF mode in similar periods was also identified by FAIMON *et al.* (2006) or LANG *et al.* (2025) in the Císařská Cave in the Moravian Karst. However, this study showed a slightly different duration of both modes. Although the duration of UAF mode was reduced to a single period from November to February (relatively following the winter season), the period of DAF mode was extended and covered almost all spring and half of fall (Figs. 2c and 3c). The expansion of DAF mode duration could be a consequence of the rise in external air temperature at a global scale over the last few decades, as described in numerous studies, e.g. BRÁZDIL *et al.* (2009), Diaz and Llanos-Garrido (2025), or Liu and Li (2025). Based on the monitoring site positions, different  $T_{CWS}^{cave}$  values were identified in (1) UBP sites (DC, A-S, SH, and ES sites) and (2) LBP sites (A-E, S, SS, and MC sites) during the period with a standard visiting route (May 2023 to May 2024).

### The extent of wall surface temperatures

$T_{CWS}^{cave}$  range from 9.2 to 11.8 °C found in EVB of the Balcarka Cave represents a relatively narrow temperature interval roughly consistent with the values of 8.7 to 13.6 °C reported by LANG *et al.* (2025) from the Cisařská Cave. It results from similar position of both caves near the village of Ostrov u Macochy in the northern part of the Moravian Karst. In contrast, these temperatures are absolutely incomparable with extreme temperatures reaching -8.8 °C measured by STŘEDOVÁ *et al.* (2014) in the Kateřinská Cave, also situated in the Moravian Karst. However, similar values (about 15 °C) were reported by AZÚA-BUSTOS *et al.* (2009) from a cave located in the coastal range of the Atacama Desert in Chile. Therefore, it is necessary to consider various factors divided into two main groups. The first group covers factors associated with the cave itself and includes cave geometry or the number of entrances. These factors play an important role in cave airflow pathways and allow the formation of specific microclimatic conditions, including slightly different  $T_{CWS}^{cave}$  in remote/hidden cave passages. The second group represents factors associated with local climate (air temperature, humidity, etc.). This comparison indicates that the Balcarka Cave belongs to caves with rather dynamic character (approaching the ideal dynamic cave).

### Spatial distribution of wall surface temperature

Comparison of the mean values measured at LBP/UBP sites during individual campaigns showed that temperatures observed at LBP sites exceeded those at UBP sites by up to 1.3 °C (Figs. 2a, b and 3a, b). This temperature imbalance was caused by the difference in temperatures of the cave airflow. During DAF mode, warm external air flowing through UBP sites was cooled by the cave walls at LBP sites. In contrast, cool external air flowing through LBP sites was heated by the cave walls at the UBP sites in UAF mode (LUETSCHER *et al.*, 2008). Despite the relatively complex evolution of all  $T_{CWS}^{cave}$  time series, almost synchronous surface temperatures between the right and left walls were identified at individual monitoring sites. On the other hand, some campaigns showed sites with slight temperature fluctuations between right/left walls, reaching up to 0.14 °C. The same behavior was also described, for example, by AZÚA-BUSTOS *et al.* (2009) for the Coastal Cave (Chile), where temperature differences between eastern and western cave walls corresponded to first tenths of °C. However, based on the IR thermometer relative error of  $\pm 4.25\%$ , temperature differences mentioned above can be considered negligible. In principle, the air circulation in the cave environment could be derived from a model of turbulent fluid motion in a channel with different flow rates in its central part and near the walls. In this context, however, the width of a cave corridor plays a key role. In the case of temperatures measured in EVB, a similarity of  $T_{RW}^{cave}/T_{LW}^{cave}$  values indicate that the central parts of the cave corridors/chambers represent preferential paths for the cave airflow. In contrast, the contact of flowing air with cave walls would lead to their warming or cooling depending on respective ventilation mode. This mechanism was observed, for example, by LANG *et al.* (2025) in the Cisařská Cave, where the cave air flowing through narrower corridors caused relatively higher temperature differences (up to 0.7 °C) between the surfaces of the right/left walls.

### Seasonality of wall surface temperature

An almost 1.5-year-long monitoring allowed the identification of  $T_{CWS}^{cave}$  evolution during regimes with (i) a standard visiting route and (ii) a modified visiting route as a result of flooding of some cave passages. The first regime, including seasonal monitoring, showed different trends of  $T_{CWS}^{cave}$  based on the actual ventilation mode. The conceptual model of individual ventilation paths operating during both DAF and UAF modes is depicted in Figure 4.

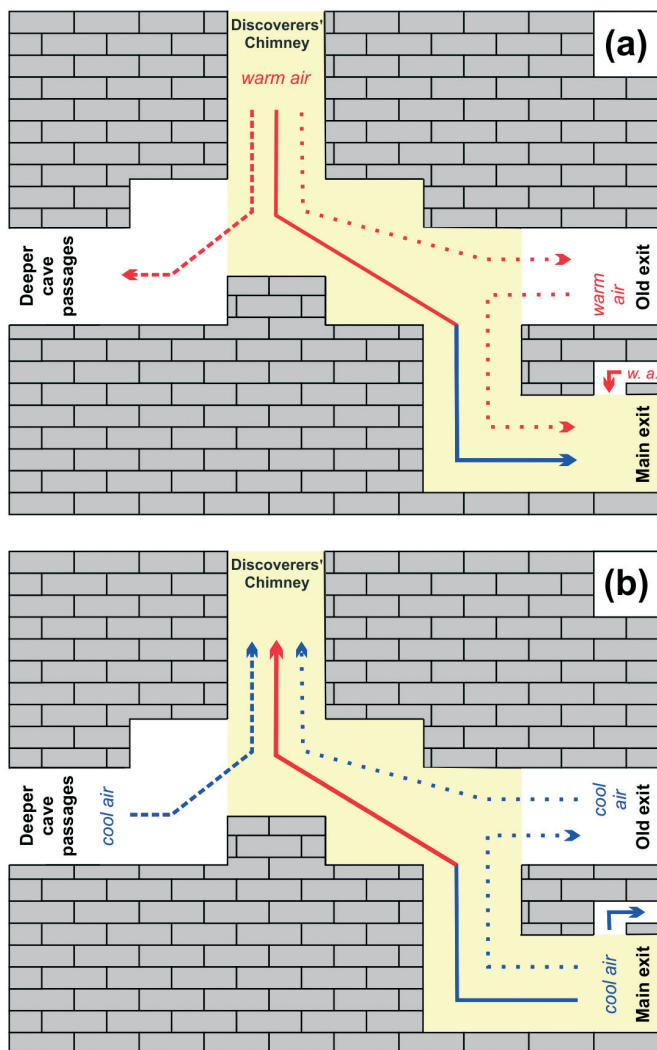


Fig. 4. Conceptual model of the Exit ventilation branch (yellow color) in the Balcarka Cave with marked ventilation paths under DAF (a) and UAF (b) ventilation mode. Individual lines correspond to the main ventilation path of the branch (full lines) and additional paths from/to deeper cave passages (dashed lines) and the Old exit (dotted lines). Line colors represent the transport of warm air (red) and cool air (blue).

Obr. 4. Konceptní model Výstupní ventilační větve (žlutá barva) v jeskyni Balcarka s vyznačenými ventilačními cestami v DAF (a) a UAF (b) módu ventilace. Jednotlivé linie odpovídají hlavním ventilačním cestám větve (plné linie) a vedlejším cestám z/do hlubších částí jeskyně (čárkované linie) a Starého východu (tečkované linie). Barvy linií představují transport teplého vzduchu (červená) a chladného vzduchu (modrá).

During DAF mode, the warm external air was sucked into EVB through the Discoverers' Chimney and heated UBP sites (Fig. 4a). This mechanism is clearly evident in the period from July to November 2023, when  $T_{CWS}^{cave}$  increased from the initial values of about 10.5 °C up to 11.8 °C (Fig. 2a, b). As the air flowed through individual sites of EVB, it was gradually cooled by cave walls, which led to a slightly cooler air at LBP sites. However, these sites were also heated by an additional portion of warm external air flowing into the cave through a window in the Museum Chamber ceiling, which was installed as an opening for bats. It caused a rapid increase in  $T_{CWS}^{cave}$  values from 9.9 °C in July up to 11.8 °C in August, followed by a plateau with the mean value of 11.0 °C in the period from September to November (Fig. 3a, b). Such a plateau indicates a switch in temperature increases or decreases, and therefore, this period could also be included in the transitional mode. Such expansion of the transitional mode was confirmed by LANG *et al.* (2015b), who estimated switching  $|\Delta T|$  in the Balcarka Cave in the range of 0.4 to 3.2 °C. In contrast to DAF mode, a completely different situation occurred during UAF mode, when cool external air entered EVB through the Main exit (Fig. 4b). Transport of cool air led to a decrease of  $T_{CWS}^{cave}$  values at LBP sites down to 9.2 °C in March 2024 (Fig. 3a, b). During its subsequent transfer towards the Discoverers' Chimney, the cave air was gradually heated by the cave walls and  $T_{CWS}^{cave}$  minima at UBP sites were higher by 1.2 °C (Fig. 2a, b).

### Factors influencing wall surface temperature

Since airflow represents the main parameter affecting  $T_{CWS}^{cave}$  evolution, changes in cave airflow could lead to disruptions of a relatively simple seasonal  $T_{CWS}^{cave}$  pattern. In this context, two examples of such phenomena, both naturally and anthropogenically induced, appeared in the  $T_{CWS}^{cave}$  time series from EVB. The first of them appeared in the 2023 summer season and was associated with ventilation mode switch as a result of a short-term  $T_{air}^{ext}$  decrease of almost 25 °C. Based on the mean  $T_{air}^{cave}$  in the homothermic zone being 9.8 °C (PTÁČNÍKOVÁ, 2025), it corresponded to a decrease of  $\Delta T$  from 23.0 to -1.9 °C (Fig. 3c) and to switching the airflow direction to UAF mode. However, the short period with negative  $\Delta T$  values (~ 28 hours), representing the presence of UAF mode, indicates that the mode switching was achieved at non-zero  $\Delta T$ . This phenomenon was published by various authors, e.g. de FREITAS *et al.* (1982) or FAIMON *et al.* (2012). LANG *et al.* (2015b) estimated the switching  $\Delta T$  by modeling in the range of 0.4 to 3.2 °C and interpreted it as a result of non-uniform distribution of temperatures, humidity, and CO<sub>2</sub> concentrations throughout the cave (FAIMON and LANG, 2013, SÁNCHEZ-CAÑETE *et al.*, 2013). Subsequent transport of cooler cave air during UAF mode then decreased  $T_{CWS}^{cave}$  values at all monitoring sites by up to 1.4 °C (Figs. 2a, b and 3a, b). Note that individual sites were cooled by air from different sources represented by (i) passages near the Main exit (LBP sites) and (ii) deeper cave passages (UBP sites). Subsequent switch back to DAF mode was associated with  $T_{CWS}^{cave}$  return to natural values, exceeding the initial values at LBP sites (Fig. 3a, b). Another period with an unexpected switch of ventilation mode occurred in April 2024, when a temperature-stable period with  $T_{air}^{ext}$  of about 23 °C was replaced by ten days with  $T_{air}^{ext}$  between 10.0 and -3.0 °C (Figs. 2c and 3c). In contrast to UAF mode interval in summer 2023, relatively constant  $T_{CWS}^{cave}$  followed after repeated switching to DAF mode at the end of April 2024. The reason was that long-term thermal stability of wall surface interrupted by a ten-day period with a distinct mode is not long enough for a significant  $T_{CWS}^{cave}$  modification. To summarize, the mechanism of ventilation mode switching is often used to describe the evolution of microclimatic parameters (e.g. LANG *et al.*, 2015a).

The second phenomenon distorting cave airflow was a modification of the visiting route due to cave floor damage in LBP by torrential rain on 21 June 2024. It resulted in a shortened visiting route and temporary replacement of the Main exit by the Old exit. The use of the Old exit on the visiting route created an additional ventilation path. However, the effect of this path on the  $T_{CWS}^{cave}$  values at individual monitoring sites differed according to

their position in EVB. While LBP sites showed no  $T_{CWS}^{cave}$  changes (differences were within the specified accuracy of the sensor), significant decreases/increases of  $T_{CWS}^{cave}$  in the range of 1.7 °C were observed at UBP sites (Fig. 2a, b). Since the ventilation paths during DAF mode are not associated with transport of cool air at UBP sites (Fig. 4a), it is obvious that the periods with  $T_{CWS}^{cave}$  decreases correspond to UAF mode. Moreover, it confirms the hypothesis of ventilation mode switching at increased  $\Delta T$  values presented by LANG *et al.* (2015b). According to  $T_{CWS}^{cave}$  evolution at DC/ES sites, sources of cool air were determined. The absence of a temperature decrease at ES site in June indicates transport from deeper cave passages. On the contrary, relatively constant values at ES site in August indicate air transport from the exterior through the Old exit.

## IMPLICATIONS

$T_{CWS}^{cave}$  represents a parameter potentially usable in various research areas of cave microclimatology. It controls microclimatic processes in cave systems, such as water vapor condensation on cave walls (e.g. SARBU and LASCU, 1997; DE FREITAS and SCHMEKAL, 2006) or determination of paleotemperatures from autochthonous cave deposits during paleoclimatic reconstructions (FAIRCHILD *et al.*, 2006). However, the mean  $T_{CWS}^{cave}$  value measured in EVB of about 10.5 °C would lead to a deviation of 0.4 °C. Based on LANG *et al.* (2025), such deviation is at the limit of applicability for common karstological interpretations (e.g. paleoenvironmental reconstructions) and even exceeds the limit for environmental-karstological interpretations (e.g. water vapor condensation). Therefore, contact methods are commonly used for temperature monitoring of cave walls. Moreover, LANG *et al.* (2025) also described a significant effect of settings of the IR thermometer, especially the emissivity degree. An experimental test of this effect showed a relatively rapid  $T_{CWS}^{cave}$  decrease by ~ 1.4 °C between emissivity degrees of 0.95 and 0.85. On the other hand, an advantage of a non-contact IR thermometer is its ability to measure  $T_{CWS}^{cave}$  in inaccessible cave passages (e.g. ceilings or chasms). It indicates that a combination of both IR and contact thermometer is required for mapping of  $T_{CWS}^{cave}$  patterns across the cave. In addition to CO<sub>2</sub> concentrations or radon activity in cave atmosphere,  $T_{CWS}^{cave}$  was also confirmed as an indicator of cave airflow. Moreover, it appears to be a suitable indicator of switching between DAF and UAF modes not only within the limits of summer and winter seasons, but especially during their peak phases. However, this approach is limited especially by the geometry of monitored cave and requires relatively simple cave systems with dynamic air circulation that allow distinct changes in  $T_{CWS}^{cave}$  pattern based on airflow variations. In large cave systems, this method could be applied only to separate ventilation branches, as documented in the example of EVB in the Balcarka Cave.

## CONCLUSIONS

The use of wall surface temperature for estimating changes in cave airflow was studied in the Exit ventilation branch of the Balcarka Cave, a dynamic cave in the Moravian Karst (Czech Republic), over a one-year period, extended by an additional summer season. Long-term data of external/cave air temperature confirmed dynamic character of the cave airflow comprising (1) downward airflow (DAF) and (2) upward airflow (UAF) ventilation modes. However, the stability of these modes was disrupted by periods of switching between DAF/UAF modes, representing the transitional ventilation mode, and by short periods in which the opposite modes occurred contrary to the long-term prevailing mode. Monitoring of the wall surface temperature in the ventilation branch identified both (i) spatial and (ii) temporal distributions. Despite a relatively narrow range of measured values, the mean temperatures at sites in the lower part of the ventilation branch were significantly higher than those at sites in the upper branch part. Comparison of data from individual monito-

ring campaigns revealed seasonality of the wall surface temperature. During DAF mode, warm external air entering the cave through the Discoverers' Chimney (upper part of the ventilation branch) or the window in the Museum Chamber ceiling (lower part of the ventilation branch) contributed to a general temperature increase. During UAF mode, transport of cool air from the exterior through the Main exit (lower part of the ventilation branch) and from deeper cave passages (upper part of the ventilation branch) led to a significant decrease in temperature. On the other hand, the study has shown that short-term changes in cave ventilation associated, for example, with ventilation mode switching or visiting route modification, may radically influence the wall surface temperatures. Therefore, temperature changes could indicate changes in the ventilation mode. Results of this study could be of interest to karstologists and environmentalists for more precise estimates of the extent of ventilation modes in caves.

## SOUHRN

Teplota povrchu jeskynní stěny je výhradně řízena výměnou vzduchu mezi externí a jeskynní atmosférou a může tak poskytovat informace o změnách proudění vzduchu v rámci jednotlivých ventilačních větví jeskyně. Pro studium tohoto fenoménu byla zvolena Výstupní ventilační větev jeskyně Balcarka v Moravském krasu. Sezónní vývoj teplotního rozdílu mezi externí a jeskynní atmosférou prokázal přítomnost sestupného proudění (DAF mód) v letních měsících a vzestupného proudění (UAF mód) v zimních měsících. K přepínání mezi oběma módy, označovanému jako přechodný mód, docházelo v průběhu pozdního podzimu a na počátku jara, avšak bylo identifikováno i ve vrcholných obdobích DAF a UAF módu. Monitoring teploty povrchů jeskynních stěn odhalil významnou prostorovou distribuci teploty v rámci Výstupní ventilační větve s vyššími hodnotami v místech situovaných v nižších pasážích větve a nižšími hodnotami v místech položených ve vyšších pasážích větve. Uvedená distribuce je výsledkem transferů tepla mezi jeskynním vzduchem a stěnami během jednotlivých ventilačních módů. Zatímco v DAF módu přispívá teplý externí vzduch k teplotnímu nárůstu, významný pokles teplot je důsledkem chladného externího/jeskynního vzduchu v UAF módu. Model může být narušen krátkodobými změnami ventilace indukovaných jak přírodními faktory (přepnutí ventilačního módu), tak i antropogenními faktory (úprava návštěvní trasy). Studium tohoto fenoménu i v dalších ventilačních větvích jeskyně Balcarka může přispět ke kompletnímu popisu ventilačního režimu celého jeskynního systému.

## ACKNOWLEDGEMENTS

The research was supported by institutional funding from Masaryk University (Brno, Czech Republic). The authors are grateful to the employees of the Balcarka Cave for their support, as well as Dr. Pavel Pracný and Dr. Jiří Rez for critical reading the manuscript. Filip Chalupka and Pavel Kalenda are thanked for their constructive reviews, which greatly improved the article.

## REFERENCES

- AZÚA-BUSTOS, A., GONZÁLEZ-SILVA, C., MANCILLA, R. A., SALAS, L., PALMA R. E., WYNNE, J. J., MCKAY, C. P., VICUÑA, R., 2009: Ancient Photosynthetic Eukaryote Biofilms in an Atacama Desert Coastal Cave. - *Environmental Microbiology*, 58, 485-496.
- BADINO, G., 2010: Underground meteorology - "What's the weather underground?". - *Acta Carsologica*, 39, 427-448.
- BALDINI, J. U. L., McDERMOTT, F., HOFFMANN, D. L., RICHARDS, D. A., CLIPSON, N., 2008: Very high-frequency and seasonal cave atmosphere PCO<sub>2</sub> variability: Implications for stalagmite growth and oxygen isotope-based paleoclimate records. - *Earth and Planetary Science Letters*, 272, 118-129.

- BANNER, J. L., GUILFOYLE, A., JAMES, E. W., STERN, L. A., MUSGROVE, M., 2007: Seasonal variations in modern speleothem calcite growth in Central Texas, USA. - *Journal of Sedimentary Research*, 77, 615-622.
- BATIOT-GUILHE, C., SEIDEL, J. L., JOURDE, H., HÉBRARD, O., BAILLY-COMTE, V., 2007: Seasonal variations of CO<sub>2</sub> and <sup>222</sup>Rn in a Mediterranean sinkhole spring (Causse d'Aumelas, SE France). - *International Journal of Speleology*, 36, 1, 51-56.
- BRÁZDIL, R., CHROMÁ, K., DOBROVOLNÝ, P., TOLASZ, R., 2009: Climate fluctuations in the Czech Republic during the period 1961-2005. - *International Journal of Climatology*, 29, 2, 223-242.
- BUECHER, R. H., 1999: Microclimate Study of Kartchner Caverns, Arizona. - *Journal of Cave and Karst Studies*, 61, 108-120.
- DE FREITAS, C. R., LITTLEJOHN, R. N., CLARKSON, T. S., KRISTAMENT, S., 1982: Cave climate: assessment of airflow and ventilation. - *Journal of Climatology*, 2, 383-397.
- DE FREITAS, C. R., LITTLEJOHN, R. N., 1987: Cave climate: assessment of heat and moisture exchange. - *International Journal of Climatology*, 7, 553-569.
- DE FREITAS, C. R., SCHMEKAL, A., 2006: Studies of condensation/evaporation processes in the Glowworm Cave, New Zealand. - *International Journal of Speleology*, 35, 2, 75-81.
- DÍAZ, J. A., LLANOS-GARRIDO, A., 2025: When spring becomes summer: global warming modifies seasonal patterns of thermoregulatory behaviour in a heliothermic lizard. - *Journal of Thermal Biology*, 133, 104243.
- DUEÑAS, C., FERNÁNDEZ, M. C., CAÑETE, S., 2005: <sup>222</sup>Rn concentrations and the radiation exposure levels in the Nerja Cave. - *Radiation Measurements*, 40, 630-632.
- DUEÑAS, C., FERNÁNDEZ, M. C., CAÑETE, S., PÉREZ, M., GORDO, E., 2011: Seasonal variations of radon and the radiation exposure levels in Nerja cave, Spain. - *Radiation Measurements*, 46, 1181-1186.
- FAIMON, J., ŠTELCL, J., SAS, D., 2006: Anthropogenic CO<sub>2</sub>-flux into cave atmosphere and its environmental impact: A case study in the Cisařská Cave (Moravian Karst, Czech Republic). - *Science of the Total Environment*, 369, 231-245.
- FAIMON, J., TROPPOVÁ, D., BALDÍK, V., NOVOTNÝ R., 2012: Air circulation and its impact on microclimatic variables in the Cisařská Cave (Moravian Karst, Czech Republic). - *International Journal of Climatology*, 32, 599-623.
- FAIMON, J., LANG, M., 2013: Variances in airflows during different ventilation modes in a dynamic U-shaped cave. - *International Journal of Speleology*, 42, 2, 115-122.
- FAIRCHILD, I. J., SMITH, C. L., BAKER, A., FULLER, L., SPÖTL, C., MATTEY, D., MCDERMOTT, F., 2006: Modification and preservation of environmental signals in speleothems. - *Earth-Science Reviews*, 75, 1-4, 105-153.
- FRISIA, S., FAIRCHILD, I. J., FOHLMEISTER, J., MIORANDI, R., SPÖTL, C., BORSATO, A., 2011: Carbon massbalance modeling and carbon isotope exchange processes in dynamic caves. - *Geochimica et Cosmochimica Acta*, 75, 380-400.
- GREGORIĆ, A., VAUPOTIĆ, J., ŠEBELA, S., 2013: The role of cave ventilation in governing cave air temperature and radon levels (Postojna Cave, Slovenia). - *International Journal of Climatology*, 34, 5, 1488-1500.
- KOTEK, M., GRIESER, J., BECK, C., RUDOLF, B., RUBEL, F., 2006: World map of the Köppen-Geiger climate classification updated. - *Meteorologische Zeitschrift*, 15, 3, 259-263.
- KOWALCZK, A. J., FROELICH, P. N., 2010: Cave air ventilation and CO<sub>2</sub> outgassing by radon-222 modeling: How fast do caves breathe? - *Earth and Planetary Science Letters*, 289, 209-219.
- LANG, M., FAIMON, J., EK, C., 2015a: A case study of anthropogenic impact on the CO<sub>2</sub> levels in low-volume profile of the Balcarka Cave (Moravian Karst, Czech Republic). - *Acta Carsologica*, 44, 1, 71-80.
- LANG, M., FAIMON, J., EK, C., 2015b: The relationship between carbon dioxide concentration and visitor numbers in the homothermic zone of the Balcarka Cave (Moravian Karst) during a period of limited ventilation. - *International Journal of Speleology*, 44, 2, 167-176.
- LANG, M., FAIMON, J., KEJÍKOVÁ, S., 2017: The impact of door opening on CO<sub>2</sub> levels: A case study from the Balcarka Cave (Moravian Karst, Czech Republic). - *International Journal of Speleology*, 46, 3, 345-358.
- LANG, M., FAIMON, J., GREGOROVÁ, M., ŠTELCL, J., CHALUPKA, F., 2025: Testing the applicability of a non-contact IR thermometer for wall surface temperature measurements in cave environment: A case study from the dynamic Cisařská Cave (Moravian Karst). - *Acta Carsologica*. In review.
- LIU, T.-Y., LI, Z.-Y., 2025: Does global warming affect the ecological surplus? - *Journal of Nature Conservation*, 88, 127015.
- LUETSCHER, M., JEANNIN, P.-Y., 2004: Temperature distribution in karst systems: the role of air and water fluxes. - *Terra Nova*, 16, 6, 344-350.
- LUETSCHER, M., LISMONDE, B., JEANNIN, P.-Y., 2008: Heat exchanges in the heterothermic zone of a karst system: Monlesi Cave, Swiss Jura Mountains. - *Journal of Geophysical Research*, 113, 13 p.
- MINEO, S., PAPPALARDO, G., 2021: Rock Emissivity Measurement for Infrared Thermography Engineering Geological Applications. - *Applied Sciences*, 11, 3773.

- OUHRABKA, V., 2025: An overview of show caves and other underground objects under the care of the Cave Administration of the Czech Republic. – In: Šimečková, B. (Ed.): Show caves 2024. A yearbook of the Cave Administration of the Czech Republic, 10–11, Cave Administration of the Czech Republic. Průhonice, Czech Republic.
- PFLITSCH, A., PIASECKI, J., 2003: Detection of an airflow system in Niedzwiedzia (Bear) Cave, Kletno, Poland. – *Journal of Cave and Karst Studies*, 65, 160–173.
- PTÁČNÍKOVÁ, T., 2025: Sezónní variace teploty a relativní vlhkosti v jeskyni Balcarka (Moravský kras). Master's thesis. – MS, Faculty of Education, Masaryk University, Brno.
- SÁNCHEZ-CAÑETE, E. P., SERRANO-ORTIZ, P., DOMINGO, F., KOWALSKI, A. S., 2013: Cave ventilation is influenced by variations in the CO<sub>2</sub>-dependent virtual temperature. – *International Journal of Speleology*, 42, 1, 1–8.
- SARBU, S. M., LASCU, C., 1997: Condensation corrosion in Movile Cave, Romania. – *Journal of Cave and Karst Studies*, 59, 3, 99–102.
- SPÖTL, C., FAIRCHILD, I. J., TOOTH, A. F., 2005: Cave air control on dripwater geochemistry, Obir Caves (Austria): Implications for speleothem deposition in dynamically ventilated caves. – *Geochimica et Cosmochimica Acta*, 69, 2451–2468.
- STUMM, W., MORGAN, J. J., 1996: *Aquatic chemistry: chemical equilibria and rates in natural waters*, 3<sup>rd</sup> Edition. – Wiley-Interscience, New York, 1040 p.
- STREDOVÁ, H., STREDA, T., VYSOUDIL, M., 2014: Cave rock surface temperature evaluation using non-contact measurement methods. – *Acta Carsologica*, 43, 2-3, 257–268.
- ŽDÍMAL, V., 2014: Proudění vzduchu v Ledové chodbě jeskyně Piková dáma, Moravský kras (Česká republika). – *Slovenský kras*, 52, 1, 45–54.
- ŽDÍMAL, V., 2015: Podmínky pro proudění vzduchu v Ledové chodbě jeskyně Piková dáma. – *Fyzickogeografický sborník*, 13, 14–17.